Laboratory study on the penetration resistance and bearing capacity of the pile driven by vibratory pile driving

Shunsuke Moriyasu[1], M. Aizawa[2], T. Matsumoto[3],
Y. Yamakuri[4], S. Suko[3] and S.-I. Kobayashi[3]

[1] Steel Structure research lab., Nippon Steel & Sumitomo Metal Corp., 20-1, Shintomi, Futtsu, Chiba, 293-8511, Japan.
[2] Toyama Prefecture, Japan (former student of Kanazawa University)
[3] Graduate School of Natural Science and Technology, Kanazawa University, Kakuma, Kanazawa, Ishikawa, 920-1192, Japan.
[4] Ph.D student at the Graduate School of Natural Science and Technology, Kanazawa University, Kakuma, Kanazawa, Ishikawa, 920-1192, Japan.

ABSTRACT

In a series of laboratory tests, the penetration resistance and bearing capacity of a model pile driven by a vibratory hammer was investigated by comparing it with pile performances conducted by different piling methods; push-in and surging. It was indicated that vibratory pile driving and surging generated contractancy of the soil surrounding the pile, and these methods decreased penetration resistance both in dry and saturated sand conditions. Based on the measured pore water pressures, it was found that the contractancy generated by the pile installed by vibratory driving and surging prevented dilation during the static load tests after the pile installation process, while the pile installed by push-in showed dilation of the soil surrounding the pile.

Keywords: pile foundation; laboratory test; vibratory pile driving; push-in; surging; pore water pressure

1 INTRODUCTION

Vibratory pile driving can install a pile with lower ground vibration and noise than the conventional impact hammer method. However, vibratory pile driving is not widely employed, because the bearing capacity of the pile driven by vibratory hammer has not been fully clarified. Hence, in order to clarify the bearing capacity of the vibratory driven pile, a series of laboratory experiments was carried out. The experiments focused on the relationships between pile penetration behavior and bearing capacity. The performance of the vibratory driven pile was compared with performance of piles installed by different piling methods; push-in and surging.

2 EXPERIMENT DESCRIPTION

First, in a pile penetration test (PPT), a model pile was installed into a dry or saturated model sand ground by push-in, surging (repetition of 2 mm push-in stroke and 1 mm pull-out stroke), or vibration. After the pile reached a depth of 400 mm, a static load test (SLT) was conducted to obtain the load-settlement behavior of the pile. Table 1 shows the experimental cases and conditions.

Fig. 1(a) shows the model pile. An open-ended aluminum pipe with an outer diameter of 32 mm, a thickness of 1.3 mm, and a length of 595 mm was used for the model pile. To obtain the distribution of axial forces, strain gauges were attached to the pile shaft at six different levels.

Table 1. Experimental cases and conditions.

Case No.	1	2	3	4	5	6
Model ground	Dry	Dry	Dry	Saturated	Saturated	Saturated
Relative density, D_r (%)	79.9	79.9	80	69.5	64.3	69.5
Dry density, ρ_d (t/m^3)	1.568	1.568	1.568	1.538	1.524	1.538
Penetration method in PPT	Push-in	Surging	Vibration	Push-in	Surging	Vibration
Penetration speed during PPT (mm/s)	0.2	0.2	-	0.2	0.2	-
Penetration speed during SLT (mm/s)	0.1	0.1	0.1	0.1	0.1	0.1
Vibration frequency (Hz)	-	-	20Hz to 35Hz	-	-	15Hz to 20Hz

The material of the model ground was silica sand #6, which has the physical properties listed in Table 2. A rigid cylindrical soil container with a diameter of 566 mm and a height of 580 mm was used. The relative density, D_r, of the ground was D_r = 80 % and D_r = 70 % for dry and saturated ground, respectively.

Fig. 1(b) shows the experimental set-up. During PPT, the pile was installed by a motor jack for push-in and surging, or a vibratory hammer for vibration (a weight of 300 N, maximum frequency of 60 Hz). During SLT, in all cases, the pile head was pushed by the jack.

In the cases of saturated ground, five pore water pressure transducers were buried at different depths and horizontal distances from the pile, as shown in Fig. 2.

To investigate the mechanical properties of the sand, monotonic and cyclic consolidated undrained (CU) shear tests were carried out. Fig. 3 shows the relationship between the axial strain, ε_a, and the deviatoric stress, q. It is seen that ε_a increases with the number of cyclic loadings, with a constant range of q. In addition, the excess pore water pressure during cyclic loading was higher than that in monotonic loading. These results indicate that cyclic shearing enhances the contractancy of the sand. The soil behavior is referred to to discuss the experiment results later in this paper.

3 EXPERIMENT RESULT

3.1 Pile penetration test stage

Figs. 4 (a) and 5 (a) show the relationship between the pile head load, P_h, and pile head displacement, w_h. The solid line corresponds to the results of PPT, and the dashed line indicates the result of SLT. During PPT, P_h in the cases of push-in and surging were measured via a load cell placed on the pile top.

On the other hand, P_h in the case of vibration was the axial force calculated from the strains near the pile top (SG level 1), subtracting the inertial force of the pile body. The inertial force was calculated as the product of the acceleration measured near the pile top and the mass of the pile. During SLT, P_h was measured by the load cell in all cases. Figs. 4 (b) and 5 (b) show the relationship between the pile base, P_b, and w_h. Here, P_b was the axial force at SG level 6. Figs. 4 (c) and 5 (c) further show the relationship between the pile shaft friction, P_s, and w_h. P_s is the difference of P_h and P_b.

In the dry sand condition, P_s in Case 2 (surging) was smaller than that for push-in, while P_b in Case 2 was larger than that for push-in. Studies by Bolton et al. (2013) and Moriyasu et al. (2016) indicate that the cyclic shear loading in surging generated contractancy of the sand surrounding the pile, while the sand below the pile tip was compacted by the cyclic loading. In Case 3 (vibration), first, the pile was installed by the self-weight of the vibratory hammer from the ground surface. When the pile could not be penetrated by the self-weight at w_h = 75 mm, the vibration of the hammer was started to install the pile. Until the pile reached w_h = 400 mm, the frequency of the hammer was increased if the pile penetration was degraded. Fig. 4 (c) shows that P_s in the case of vibration was smaller than that in the case of Push-in. Furthermore, P_b in the case of vibration was smallest after w_h exceeded 200 mm. A possible reason for this is the generation of excess pore air pressure. Watanabe et al. (2013) found that excess pore air pressure is generated in dry sand when it is sheared very rapidly in triaxial compression testing. It is difficult to derive a definite conclusion in this stage, and further study is needed to clarify this behavior.

Table 2. Physical properties of silica sand No.6.

Soil particle density, ρ_s (t/m^3)	2.679
Min. dry density, ρ_{dmin} (t/m^3)	1.366
Max. dry density, ρ_{dmax} (t/m^3)	1.629
Max. void ratio, e_{max}	0.962
Min. void ratio, e_{min}	0.645
Average particle size, D_{50}	0.52

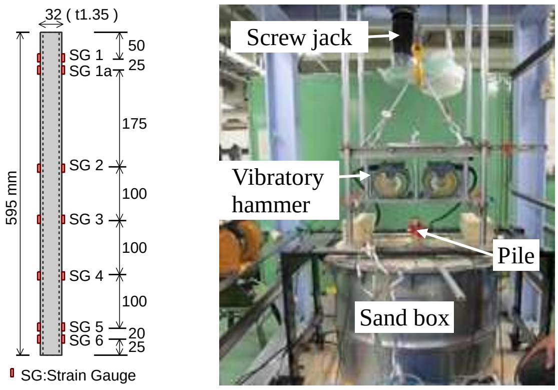

(a) Model pile. (b) Experimental set-up.

Fig. 1. Experimental apparatus.

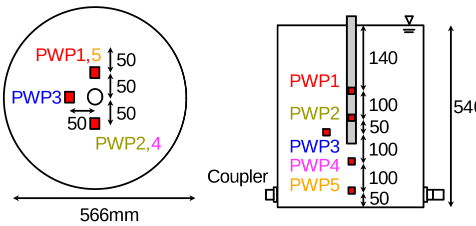

Fig. 2. Locations of pore water pressure gauges in Cases 4 to 6.

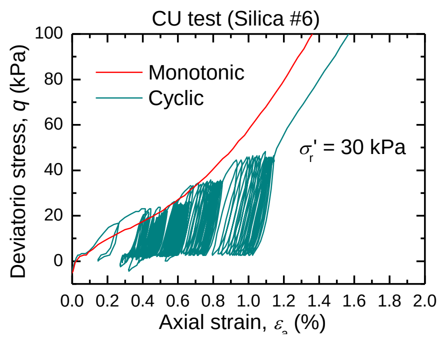

Fig. 3. Relationship between the axial strain and deviatoric stress during monotonic and cyclic CU test.

Under saturated sand condition, all pile resistances were smaller than those under dry sand condition, because the effective vertical stresses under saturated sand condition were almost half of those under dry sand condition. The values of P_s in Case 5 (surging) and Case 6 (vibration) were smaller than those in Case 4 (push-in), while the value of P_b in all cases was comparable. Additionally, in Case 6, when the pile reached w_h = 400 mm, the frequency of the hammer was increased from 17.7 Hz to 18.3 Hz to enhance pile installation. Then, P_b decreased significantly. This is related to soil liquefaction. Fig. 6 (c) shows the pore water pressure (P.W.P.), p. It was seen that p fluctuated largely when the pile tip reached a depth of 400 mm. This indicates the occurrence of soil liquefaction.

3.2 Static load test stage

As shown in Figs. 4 (a) and 5 (a), P_h in SLT during vibratory driving became much higher than P_h in the final stage of PPT (around w_h = 400 mm). On the other hand, P_h in SLT during push-in and surging was similar to P_h in the final stage of PPT.

Fig. 7 shows a comparison of the load-settlement relations. The origin of the vertical axis of Fig. 7 (i.e., pile head displacement during SLT, w_{h_SLT}) is set as w_h at the end of PPT in each case, for the purpose of comparison. The dotted point of each curve denotes the yield point in the 1st loading cycle. The yield load in Case 2 (surging) and Case 3 (vibration) was higher than that in Case 1 (push-in) under both dry and saturated sand conditions. Fig. 8 shows P_s and P_b at the yield point. Both P_s and P_b in the cases of vibration (Cases 3 and 6) were the same or higher than those in other cases.

The bottom part in Fig. 6 shows p during SLT. The vertical axis on the right-hand side corresponds to the pile head displacement during SLT, w_{h_SLT}. It can be seen from Fig. 6 (a) that the negative increment of p (i.e., positive dilation of the ground) was generated in Case 4 (push-in). Although the magnitudes of p in Case 5 and Case 6 were smaller than those in Case 4, their trends were similar to that in Case 4. A possible reason why the magnitudes were small is that cyclic shearing during PPT prevents the dilation of the ground during SLT. During PPT in Case 5 (surging), the pile penetration speed was 0.2 mm/s, and the total number of cycles was 350. The corresponding values in Case 6 (vibration) were 87 mm/s and 3800, respectively.

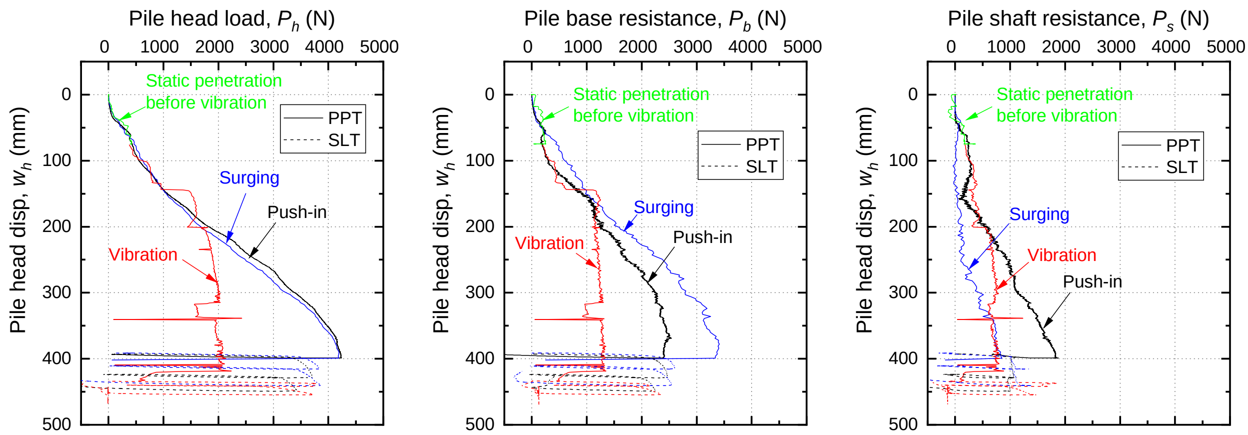

(a) Pile head (b) Pile base (c) Pile shaft

Fig. 4. Comparison of pile resistances during PPT and SLT in dry sand conditions (Cases 1 to 3).

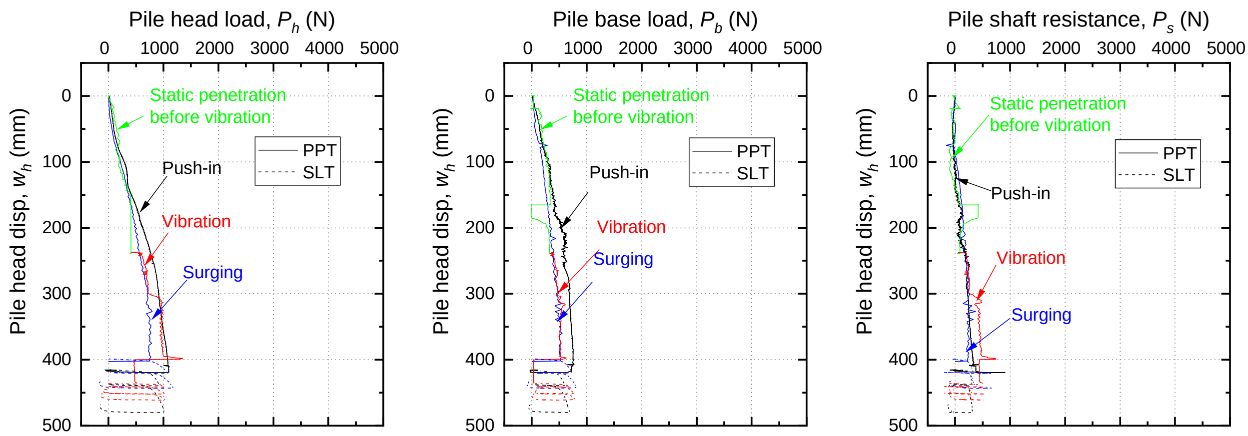

(a) Pile head (b) Pile base (c) Pile shaft

Fig. 5. Comparison of pile resistances during PPT and SLT in saturated sand conditions (Cases 4 to 6).

As shown in the above CU test, the axial strain of the sand accumulated with an increase in the number of cyclic shearing. This indicates that cyclic shearing enhanced the contractancy of sand and may prevent positive dilation. If the cyclic pile movement in Cases 5 and 6 has a similar effect in the cyclic CU test, a large number of cyclic shearing by the pile may enhance the contractancy of the pile surrounding sand. As a result, positive dilation was hardly generated during SLT. This is a possible reason why the magnitudes of *p* in Cases 5 and 6 were smaller than that in Case 4.

4 CONCLUSIONS

A series of laboratory test were carried out to clarify the bearing capacity of the pile driven by a vibratory hammer. The test compared the pile penetration resistance and bearing capacity among different piling methods, i.e., monotonic push-in, surging, and vibration under dry or saturated sand condition.

During vibratory pile driving, pore air pressure under dry sand condition and soil liquefaction under saturated sand condition were indicated. A possible reason for these behaviors is that vibratory driving generated contractancy of the sand surrounding the pile. The static load test shows that the bearing capacity of the vibratory driven pile was comparable to that of push-in and surging. Based on the response of the pore water pressure during SLT, the cyclic shearing of surging and vibratory driving prevents ground dilation.

ACKNOWLEDGEMENTS

The authors would like to express their gratitude to Mr. Shimono (Technician of Kanazawa University), Dr. Vu Ahn Tuan (former PhD student of Kanazawa University), Mr. Soichiro Suko, Ms. Syafinaz Saadon and Mr. Mayumi (former students of Kanazawa University) for their kind supports in this study.

REFERENCES

Bolton, M.D., Haigh, S.K., Shepley, P., and D'Arezzo, F.B. (2013). Identifying ground interaction mechanisms for press-in piles. Press-in Engineering 2013, Proc. 4th IPA International Workshop in Singapore, pp84-95.

Moriyasu, S., Meguro, H., Matsumoto, T., Kobayashi, S., and Shimono, S. (2016). Influence of Surging and Jack-in Pile Installation Methods on Pile Performance Observed in Model Load Tests in Dry Sand Ground. 19th Southeast Asian Geotechnical Conference & 2nd AGSSEA Conference, 621-626.

Watanabe, K. and Kusakabe, O. (2013). Reappraisal of Loading Rate Effects on Sand Behaviour in View of Seismic Design for Pile Foundations. Soils and Foundations, 53(2), 215-231.

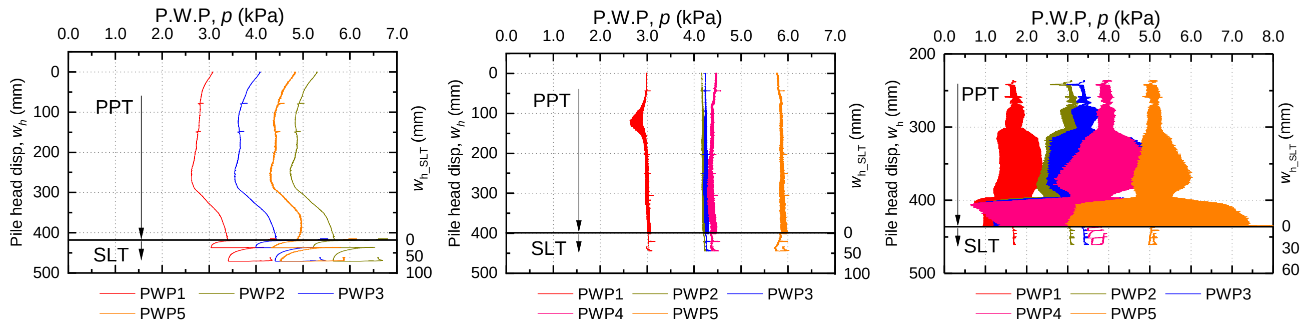

(a) Case 4 (Push-in) (b) Case 5 (Surging) (c) Case 6 (Vibration)

Fig. 6. Relationship between the pile head displacement, w_h, and the water pressure (P.W.P), p, during PPT.

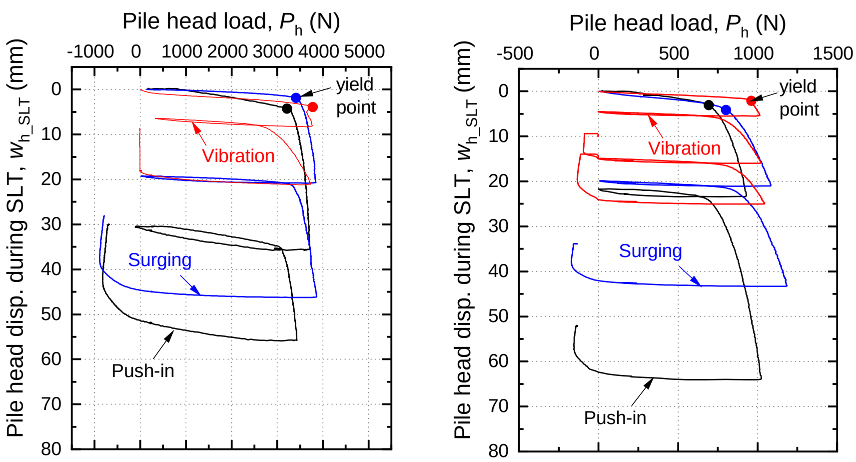

(a) Dry sand condition (case 1 to 3) (b) Saturated sand condition (case 4 to 6)

Fig. 7. Relationship between P_h and the pile head displacement during SLT, w_{h_SLT}.

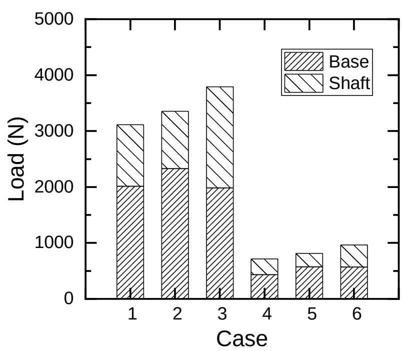

Fig. 8. Share of P_b and P_s.